JOURNAL OF AGRICULTURAL AND FOOD CHEMISTRY

pubs.acs.org/JAFC

Article

Screening, Characterization, and Mechanistic Evaluation of Angiotensin Converting Enzyme Inhibitory Peptides Derived from Milk Fermented with *Lactobacillus delbrueckii* QS306 with and without Ultrahigh-Pressure Treatment

Nan Wu, Wuhanqimuge,* and Quan Shuang*

Cite This: https://doi.org/10.1021/acs.jafc.3c03752 Read Online

ACCESS | Metrics & More | Article Recommendations

ABSTRACT: In this study, the peptides in milk fermented with *Lactobacillus delbrueckii* QS306 with and without ultrahigh-pressure treatment were identified using UPLC-Q-exactive-HF-X-MS/MS. In total, 27 novel pentapeptides with potential angiotensin converting enzyme inhibitory (ACEI) activity were screened via bioinformatic analysis, and the activities of seven novel pentapeptides were assessed. Among them, HLPLP, PYPQR, and VAPFP exhibited better IC_{50} values. Stability assessment via in vitro simulation revealed that the three pentapeptides were significantly reduced (P < 0.05) during digestion but exhibited 85% activity after digestion. HLPLP was a competitive inhibitor, while PYPQR and VAPFP were noncompetitive inhibitors of ACE. Molecular docking indicated that the three peptides could stably bind to ACE. Molecular dynamics (MD) simulation and activity verification indicated that PYPQR and VAPFP had better stability and activity. This study demonstrated that novel ACEI pentapeptides in milk fermented with *L. delbrueckii* QS306 with and without ultrahigh-pressure treatment could be considered promising candidates for controlling hypertension.

KEYWORDS: *angiotensin converting enzyme inhibitory peptides, fermented milk, molecular docking, molecular dynamics simulation*

1. INTRODUCTION

Hypertension is a multietiological, chronic disorder that can lead to dysfunctions in multiple organs, e.g., cardiovascular disease, stroke, and renal complications. Normal blood pressure is maintained at the mean systolic blood pressure (SBP) of 120 mmHg and mean diastolic blood pressure (DBP) of 80 mmHg. Hypertension is defined as the SBP ≥ 140 mmHg and DBP ≥ 90 mmHg.[1] Hypertension has become an epidemic with the third-highest disability-adjusted life years as reported by the World Health Organization.[2] More than 1 billion people worldwide suffer from hypertension, and the number could rise to 1.56 billion by 2025.[3]

The treatments for hypertension became available in the mid-19th century,[4,5] including appropriate dietary intake and medication. Angiotensin converting enzyme (ACE) inhibitors, β blockers, diuretics, angiotensin receptor blockers, and calcium channel blockers are used in the treatment of hypertension.[6] However, antihypertensive drugs have various adverse reactions. Diuretics can cause increased urinary frequency, muscle spasm, and arrhythmia. β blockers exacerbate asthma and diabetes and lead to stomach cramps, blurred vision, depression, and nightmares.[7] ACE inhibitors can cause dry cough, rash, hyperkalemia, fetal malformations, and allergic reactions.[8] Moreover, if hypertension is accompanied by other diseases, multiple drugs are administered causing adverse drug reactions. Additionally, these diseases may affect the body's response to antihypertensive drugs and may negatively affect metabolic processes. Synthetic antihypertensive drugs are considered the culprit for various side effects. Therefore, the search for natural, food-based antihypertensive drugs with no side effects is gaining momentum.

ACE is an unusual zinc dipeptidase that was reported to lack substrate specificity in vitro due to its activation by chloride.[9] ACE inhibitors were first obtained from snake venom.[10] Subsequently, multiple ACE inhibitors were discovered in food ingredients, including bovine casein, zein, gelatin, yeast, and corn.[11,12] In our previous study, we purified an ACE inhibitory (ACEI) peptide LPYPY with good activity from milk fermented by *Lactobacillus delbrueckii* QS306 via traditional separation methods.[13]

For identifying bioactive peptides from proteins, bioinformatic methods are less costly and more effective than conventional methods. BIOPEP-UWM is a bioinformatic database and PeptideRanker is a tool for analyzing the ACEI peptides in proteins. Using these tools, the simulation of protein hydrolysis, peptide activity prediction, structure−activity relationship, and prediction of physicochemical properties of peptides can be conducted.[14] In addition,

Received: June 5, 2023
Revised: September 18, 2023
Accepted: September 21, 2023

computer molecular docking is a valuable tool for screening and designing ACEI peptides and is widely used to elucidate the mechanism of interaction.[15] The evaluation of interaction energy can reveal the affinity and binding pattern between ACE and a peptide.[16]

In our previous study, we found that the ACE inhibitory activity of fermented milk increased significantly after ultra-high-pressure (UHP) treatment. Therefore, the peptides in fermented milk with and without UHP treatment were subjected to peptidomic analysis, and the activity and stability of short peptides were predicted and screened using bioinformatic tools. Screened peptides were subjected to solid-phase synthesis to determine their activity, stability, and inhibitory pathways. The ACEI peptides were identified, and the interaction between the ACEI peptides and ACE was explored using molecular docking. The stability of docking results was assesed using MD. This study identified active and stable ACEI peptides in milk fermented with *L. delbrueckii* QS306 under UHP.

2. MATERIALS AND METHODS

2.1. Materials. *L. delbrueckii* QS306 was isolated from traditionally fermented milk (yogurt fermented by herdsmen) from Xilin Gol League. ACE from rabbit lung, hippuric acid (HA), and *N*-benzoyl-Gly-His-Leu, (*N*-hippuryl-His-Leu hydrate; HHL, powder, H1635) were purchased from Sigma-Aldrich Chemical Co. (Saint Louis, MO). de Man, Rogosa, and Sharpe (MRS) medium was purchased from Guangdong Huankai Microbial Sci. & Tech. Co., Ltd. (Guangzhou, China). Simulated gastric fluid and intestinal fluid were obtained from Yuanye Biotechnology Co., Ltd. (Shanghai, China).

2.2. Preparation of Fermented Milk (FM), Ultrahigh-Pressure-Treated FM (UHP-FM), and Ultrafiltration Component. *L. delbrueckii* QS306 was grown in MRS broth at 37 °C for 24 h and was subcultured three times. Further, the cells were centrifuged at 3500 *g* for 10 min, and the cell pellet was resuspended in sterile saline water. Overall, 3% (v/v) cell suspension was added to 11% (w/v) sterile reconstituted skim milk, followed by incubation at 37 °C for 48 h to obtain FM.

FM was treated under ultrahigh pressure (HPP 600 MPa/30 L, Baotou Kefa High Pressure Tech. Co., Ltd., Baotou, China) at 400 MPa for 10 min to obtain UHP-FM. The FM and UHP-FM were adjusted to pH 4.6, followed by centrifugation at 3000*g* and 4 °C for 15 min. The supernatant was collected and adjusted to pH 8.3, followed by centrifugation at 3000*g* and 4 °C for 10 min. Further, the supernatant was placed in a 3 kDa ultrafiltration (UF) centrifuge tube (Amicon Ultra-15 mL, Millipore, Billerica), followed by centrifugation at 2500*g* and 4 °C for 20 min. Finally, the fractions with molecular weight (MW) < 3 kDa were collected.

2.3. Determination of Peptide Sequence. The fractions of FM and UHP-FM with MW < 3 kDa were subjected to desalting. The desalted samples were eluted using a UPLC-Q-exactive-HF-X-MS/MS mass spectrometer (Easy nLC 1200, Thermo Fisher Scientific Inc., Waltham, MA), and the data were analyzed using MaxQuant 1.6.1.0 software[17] and a Uniprot protein database of Uniprot-*Bos taurus* (Bovine) [9913]-46728-20201102.

2.4. Stability Prediction and Simulation of the Synthesis of Short Peptides. PeptideCutter (https://web.expasy.org/peptidecutter/) predicts the results of simultaneous hydrolysis of a protein by a single protease and multiple proteases producing peptides. PeptideCutter was used to simulate the digestion of newly identified peptides with activity scores >0.6 (http://distilldeep.ucd.ie/PeptideRanker/) and hydrophobicity >7.0.[18] Fmoc solid-phase synthesis was performed by Gil Biochemical (Shanghai, China) Co., Ltd.

2.5. ACEI Activity Assay and Peptide Inhibition Pattern. Each peptide was dissolved in boric acid buffer solution (BBS; pH 8.3), and its ACEI activity was determined as per the method described by Wu et al.[19] Each peptide (40 μL) was treated with HHL (80 μL, 0.5 mM) at 37 °C for 5 min. To this, ACE (40 μL, 0.1 U/mL) was added. The mixture was incubated at 37 °C for 60 min, followed by the addition of HCl (200 μL, 1.0 mol/L) to stop the reaction. The control included BBS (40 μL, pH 8.3) instead of peptides. The peak area of HA produced after the reaction was determined using a 10 μL reaction solution. The ACEI rate of the peptides was calculated according to the following formula

$$\text{ACE inhibition (\%)} = [(A_{\text{control}} - A_{\text{inhibitor}})/A_{\text{control}}) \times 100$$

The inhibition patterns of peptides were determined as per a previously described method[20] with slight modifications. In brief, the peptides and HHL were dissolved in 0.10 mol/L BBS. Each peptide (20 μL) was treated with 50 μL HHL (0.15625, 0.3125, 0.625, 1.25, and 2.5 mmol/L) at 37 °C for 5 min. To this, 20 μL ACE was added. The mixture was incubated at 37 °C for 65 min, followed by the addition of HCl (60 μL, 1.0 mol/L) to stop the reaction. The inhibition pattern of the peptides was determined using the Lineweaver−Burk plot. The slope of the Lineweaver−Burk line was taken as the *Y* axis, and the peptide concentration was taken as the *X* axis. The inhibition constant (K_i) was the intercept on the *X* axis.

2.6. Molecular Docking. Molecular docking was used to predict the low-energy binding mode of ligands and receptor active sites. Thus, it further explained the mechanism of binding of ACEI peptides and ACE. In Discovery Studio 2019 software, the molecular structure of short peptides was constructed. The crystal structure of ACE (PDB: 1O8A) was downloaded from the PDB (http://www.rcsb.org/) database. Except for Zn and Cl ions, all other heteroatoms were removed from the original PDB file of 1O8A, and the resulting structure was subjected to the flexible docking method of CDOCKER as implemented in DS-2019. The active coordinate site was defined as X:36.4297, Y:37.2927, and Z:42.4473, and the docking radius was 15 Å. The molecular docking results were evaluated based on the interaction sites of -CDOCKER_ENERGY, -CDOCKER_INTERACTION_ENERGY, and ACE with the peptides, as well as the type of interaction force.

2.8. In Vitro Digestion Simulation. A pepsin−trypsin in vitro system simulating gastrointestinal digestion was used according to a method described previously[21] with slight modifications. Briefly, each peptide (1 mg/mL) was treated with simulated gastric fluid (4%, pH 2) on a water bath shaker (65 rpm) at 37 °C for 2 h. Subsequently, the solution was adjusted to pH 7.5, and simulated intestinal fluid (4%, pH 7.5) was added. The solution was incubated on a water bath shaker (65 rpm) at 37 °C for 3 h, and samples were collected every 30 min. The enzymes were inactivated by heating at 95 °C for 10 min. The solution was adjusted to pH 8.3 to determine the ACEI activity. The peptide-digesting effect of the simulated gastric fluid and intestinal fluid was assessed.

2.9. Molecular Dynamics (MD). MD simulations were used to analyze the structural stability and conformational flexibility of the docked composite structures. MD simulations were performed using the GROMACS (https://www.gromacs.org) program. The AnteChamber PYthon Parser interfacE (ACPYPE) in Amber Tools v18 was used to parametrize the topology, atomic type, and charge required for small molecules. Amber99sb-ildn force field was applied to all simulations. The SPC216 water molecules were added to the dodecahedron, Na^+ and Cl^-, to balance the charge in the system to neutral, and energy minimization (EM) was performed. Further, the system was heated to 310.15 K in 1 fs time steps during the 200 ps NVT simulation, and the pressure was balanced to 1 atm in 2 fs time steps during the 100 ps NPT simulation. For the 80 ps MD simulation, a well-balanced system with constant pressure was released and constrained, and a jump algorithm was further used to perform the simulation balance of 100 ns in steps of 2 fs. The particle grid Ewald summation method with 0.16 grid spacing was used to calculate the long-distance electrostatic interaction, and the parallel LINCS method was used to constrain the hydrogen bonds during the equilibrium process. Finally, MD simulation was performed. During the simulation run, the entire trajectory was saved for analysis at a frequency of 100 ps. To evaluate the dynamic and static interactions of the complex, the MD trajectory was analyzed using the following

https://doi.org/10.1021/acs.jafc.3c03752
J. Agric. Food Chem. XXXX, XXX, XXX−XXX

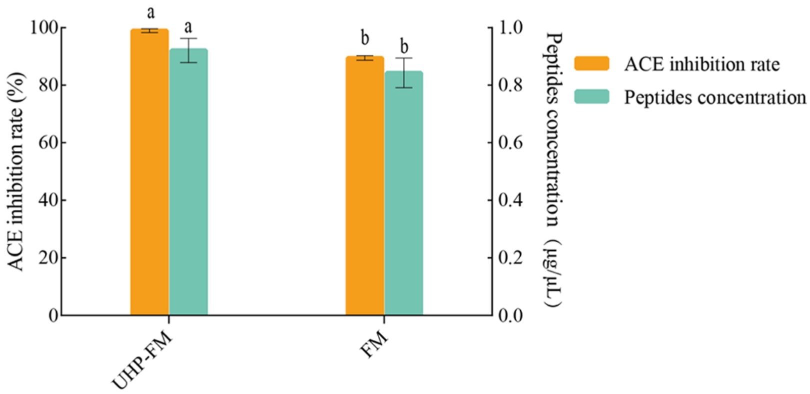

Figure 1. ACE inhibitory activities and peptide concentration of MW < 3 kDa from fermented milk before and after ultrahigh-pressure treatment.

Table 1. Screening of Pentapeptides in UHP-FM and FM Based on Hydrophobicity and Activity[a]

UniProt AC	protein	peptides	mass	activity scores	hydrophobicity (Q)	PI	sample source
A0A3Q1M5U9	kappa-casein	PHLSF	642.3	0.71	7.95	7.17	#O
		FFSDK	672.36	0.72	7.63	5.84	O
E1BBB8	transcriptional repressor GATA binding 1	PGLPN	496.26	0.64	7.75	5.96	#O
F1MCG9	diacylglycerol kinase	FLRKF	504.29	0.93	9.08	11	#O
F1MR22	polymeric immunoglobulin receptor	LDPSF	577.27	0.77	8.21	3.8	#O
P02662	α-S1-casein	YLGYL	627.33	0.74	11.17	5.52	#O
		YFYPE	667.32	0.68	10.85	4	#O
		FYPEL	759.37	0.79	10.39	4	#O
		YPELF	414.23	0.77	10.39	4	O
		VAPFP	667.32	0.82	10.31	5.49	#O
		TMPLW	554.24	0.91	9.57	5.19	#O
		FPEVF	507.28	0.8	9.56	4	#O
		APFPE	507.23	0.72	8.88	4	#O
		FRQFY	400.28	0.92	8.31	8.75	#O
		FYQLD	434.26	0.6	8.15	3.8	#O
		LFRQF	513.36	0.92	7.7	9.75	#
P02663	α-S2-casein	FPQYL	518.29	0.91	8.99	5.52	#O
		KFPQY	666.34	0.68	8.99	8.59	#
P02666	β-casein	PLPLL	426.25	0.84	11.8	5.96	#O
		YPFPG	359.18	0.96	11.28	5.52	#O
		VVPPF	438.28	0.75	10.79	5.49	#O
		HLPLP	659.34	0.75	9.68	6.74	#O
		PVEPF	349.2	0.6	9.4	4	#O
		MFPPQ	503.24	0.92	8.26	5.28	#
		PYPQR	579.27	0.65	7.84	9.18	#O
		FPPQS	477.26	0.71	7.51	5.52	#O
P80195	glycosylation-dependent cell adhesion molecule 1	FSHAF	607.28	0.91	7.04	6.74	#

[a]"#" indicates FM, and "O" indicates UHP-FM.

parameters: root-mean-square deviation (RMSD), root-mean-square fluctuation (RMSF), β factor, hydrogen bond number (H bond), free energy landscape (FEL), and binding pattern.

2.10. Calculation of Free Energy of Binding. The free energy of molecular binding is a very important physical parameter describing the affinity of a protein and ligand. In this study, the molecular mechanics Poisson−Boltzmann surface area (MM-PBSA) method was used to estimate the free energy of binding. In total, 51 snapshots were taken at 100 ps intervals from 90−95 or 95−100 ns of the MD trajectory to calculate the free energy of binding (ΔG_{bind}) using the g_mmpbsa method. The ΔG_{bind} was calculated by a combination of van der Waals (ΔG_{vdw}), electrostatic (ΔG_{ele}), polar (ΔG_{polar}), and nonpolar solvent (ΔG_{nonpol}) energies. Subsequently, the contribution of each residue to the ΔG_{bind} was determined, which was used to further explore the binding strength of important residue pairs to hit binding.

2.11. Data Statistics and Analysis. The data were expressed as mean ± standard deviation (SD). GraphPad Prism 9.0 (GraphPad Software Inc., La Jolla, CA) and Microsoft Excel 2020 (Microsoft Co.) software were used to generate graphs.

3. RESULTS AND DISCUSSION

3.1. Assessment of the ACEI Activity of Peptides. After UHP treatment, the ACE inhibitory activity of the ultrafiltration separation with MW < 3 kDa of whey in milk fermented with *L. delbrueckii* QS306 was significantly higher than that of untreated whey (Figure 1). The concentration determination and sequence analysis of the samples with MW < 3 kDa in UHP-FM and FM were performed using peptidomics, and the concentration in UHP-FM was significantly higher than that in FM. The protein source,

https://doi.org/10.1021/acs.jafc.3c03752
J. Agric. Food Chem. XXXX, XXX, XXX−XXX

relative molecular mass, potential activity score, hydrophobicity, isoelectric point, and sample source of 566 short peptides from UHP-FM and FM were analyzed, and 27 pentapeptides with activity scores >0.6 and hydrophobicity >7 kJ/mol were screened (Table 1). Further, PeptideCutter was used to predict the stability of the pentapeptides. In total, seven new peptides with good stability coexisted in FM and UHP-FM. The ACEI activity of each pentapeptide was verified after chemical synthesis (Table 2). At a peptide concentration

Table 2. Pentapeptide ACE Inhibitory Rate and IC_{50}

peptides	ACE inhibitory rate (%)	IC_{50} (μmol/L)
APFPE	59.18 ± 8.03	>10,000
FPPQS	74.53 ± 0.74	5757.722
HLPLP	96.58 ± 0.39	698.943
PYPQR	97.01 ± 0.60	454.0911
VAPFP	97.91 ± 0.14	10.5613
VVPPF	18.19 ± 2.24	>10,000
YPFPG	19.13 ± 9.82	>10,000

of 5 mg/mL, five pentapeptides with ACEI activity >50% were identified. The ACE semi-inhibitory concentrations of the seven pentapeptides were determined. Among them, the ACE semi-inhibitory concentrations of APFPE, VVPPF, and YPFPG were >10 mmol/L, whereas those of HLPLP, VAPFP, and PYPQR were higher. The amino acid sequence (proline, histidine, leucine, and arginine) and the hydrophobic amino acid at the C-terminal influence the ability of the peptides to bind to the active site of ACE.[22]

3.2. Determination of the ACE Inhibition Pattern of the Screened Pentapeptides.

To determine the ACE inhibition pattern, Lineweaver−Burk plots were generated. Kinetic studies were performed in the absence and presence of 100 and 200 μM of HLPLP and PYPQR peptides and the absence and presence of 10 and 60 μM of VAPFP peptides. The V_{max} of HLPLP remained unchanged; however, the K_m value was altered, which is an indication of a competitive inhibitory pattern (Figure 2A). Most of the ACEI peptides exhibited competitive inhibition patterns.[23] The K_m was 3.228 mM for the control (without peptide), whereas it was 8.818 and 25.556 mM in the presence of 100 and 200 μM HLPLP, respectively, which is indicative of the reduced affinity of the enzyme for its substrate in the presence of these peptides. Collectively, the results demonstrated that HLPLP inhibits ACE by binding to free enzymes rather than to ACE−substrate complexes. Since the inhibitory pattern of ACEI peptides was related to their structures, we assumed that these peptides might have structures similar to that of substrates. Thus, the peptides may compete with the substrates for the same interaction site on the enzyme. The K_m value of PYPQR and VAPFP remained unchanged; however, the V_{max} was altered, which is an indication of a noncompetitive inhibitory pattern (Figure 2B,C). The V_{max} was 13.323 μg/mL·min for the control (without peptide), whereas it was 7.337 and 6.631 μg/mL·min in the presence of 100 and 200 μM PYPQR, respectively, and 11.912 and 7.508 μg/mL·min in the presence of 10 and 60 μM VAPFP, respectively. This indicated that these peptides can bind to ACE to produce dead-end complexes,[24] irrespective of the substrate molecule binding to an active site on the enzyme. In addition, this indicated that these peptides and substrates bind to the enzyme at different sites, reducing the activity of the enzyme by forming enzyme−substrate−inhibitor and enzyme−inhibitor complexes. K_i indicates the binding affinity of the peptides toward ACE. The higher the K_i, the lower the affinity toward ACE.[25] K_i was 12.55, 205.6, and 77.84 μM for HLPLP, PYPQR, and VAPFP, respectively. VAPFP exhibited better inhibitory activity than HLPLP. This result did not quite conform to the inhibition curve. This is because the MW of HLPLP is greater than that of VAPFP; therefore, the molar concentration of HLPLP at the same mass concentration may be less than that of VAPFP.

3.3. In Vitro Simulated Gastrointestinal Digestion.

Bioactive peptides must survive gastrointestinal digestion and reach their targets with intact structure and activity. The resistance of PYPQR, VAPFP, and HLPLP to digestive enzymes was evaluated (Figure 3). The ACEI rates of PYPQR and VAPFP were 97.02 ± 0.64 and 97.91 ± 0.14%, respectively. After treatment with pepsin (Figure 3A), trypsin (Figure 3B), and gastrointestinal protease (Figure 3C), their ACEI rates were 91.65 ± 0.07 and 89.92 ± 0.27%, 90.41 ± 1.26 and 90.31 ± 0.27%, and 90.46 ± 1.09 and 86.92 ± 0.14%, respectively. Therefore, the ACEI activity was significantly decreased after treatment with pepsin, trypsin, and gastrointestinal protease ($P < 0.05$). After treatment with pepsin (Figure 3A), the ACEI rate of HLPLP was 96.58 ± 0.39%, and the ACEI activity was 95.66 ± 2.48% ($P > 0.05$), which did not change significantly. The ACEI rates of HLPLP after treatment with trypsin and gastrointestinal protease (Figure 3B,C) were 90.27 ± 0.45 and 88.40 ± 1.82%, respectively ($P < 0.05$), exhibiting a significant reduction. The ACEI activities of all of the peptides were significantly reduced after digestion with gastrointestinal proteases; however, their digested products exhibited >85% ACEI activity, proving that the short peptides had certain digestive resistance.

VAPFP and HLPLP have proline residues at the C-terminal. Short-chain peptides, especially those with proline at the C-terminal, are generally not easily degraded by proteases. In addition, they are absorbed more rapidly in the small intestine than free amino acids and large oligopeptides.[26] Xu et al. detected various peptides in the soybean protein hydrolysate prepared using Alcalase, where all peptides were competitive ACE inhibitors, and the short peptides IY, FF, LVF, WMY, YVVF, and LVLL could not retain their structure or activity during in vitro simulated gastrointestinal digestion.[16]

3.4. Probing the Binding Sites via Molecular Docking.

-CDOCKER_ENERGY and -CDOCKER_INTERACTION_ENERGY are indicators of the quality of the molecular docking results. -CDOCKER_ENERGY is calculated based on the strain energy of the internal ligand. -CDOCKER_INTERACTION_ENERGY is the energy of the receptor−ligand interaction, which is the energy of the nonbond interaction that exists between the protein and the ligand. The high values of these two indicators indicate good ligand−receptor interaction (good binding between the protein and the ligand). The position with the highest two indicators was selected as the optimal binding position for further analysis. The docking results of the peptides and ACE are shown in Table 3.

ACE mainly consists of three active site pockets, namely, the S1′, S1, and S2 pockets. The S1′ pocket is considered the main pocket for the interaction between ACE and the peptide and has only one amino acid residue, Glu162.[27] The S1 pocket consists of Glu384, Ala354, and Tyr523 amino acid residues. However, the S2 pocket contains five amino acid residues, including His383, Gln281, Tyr520, Gln282, and Lys511. Glu411, His383, and His387 play an important role in the

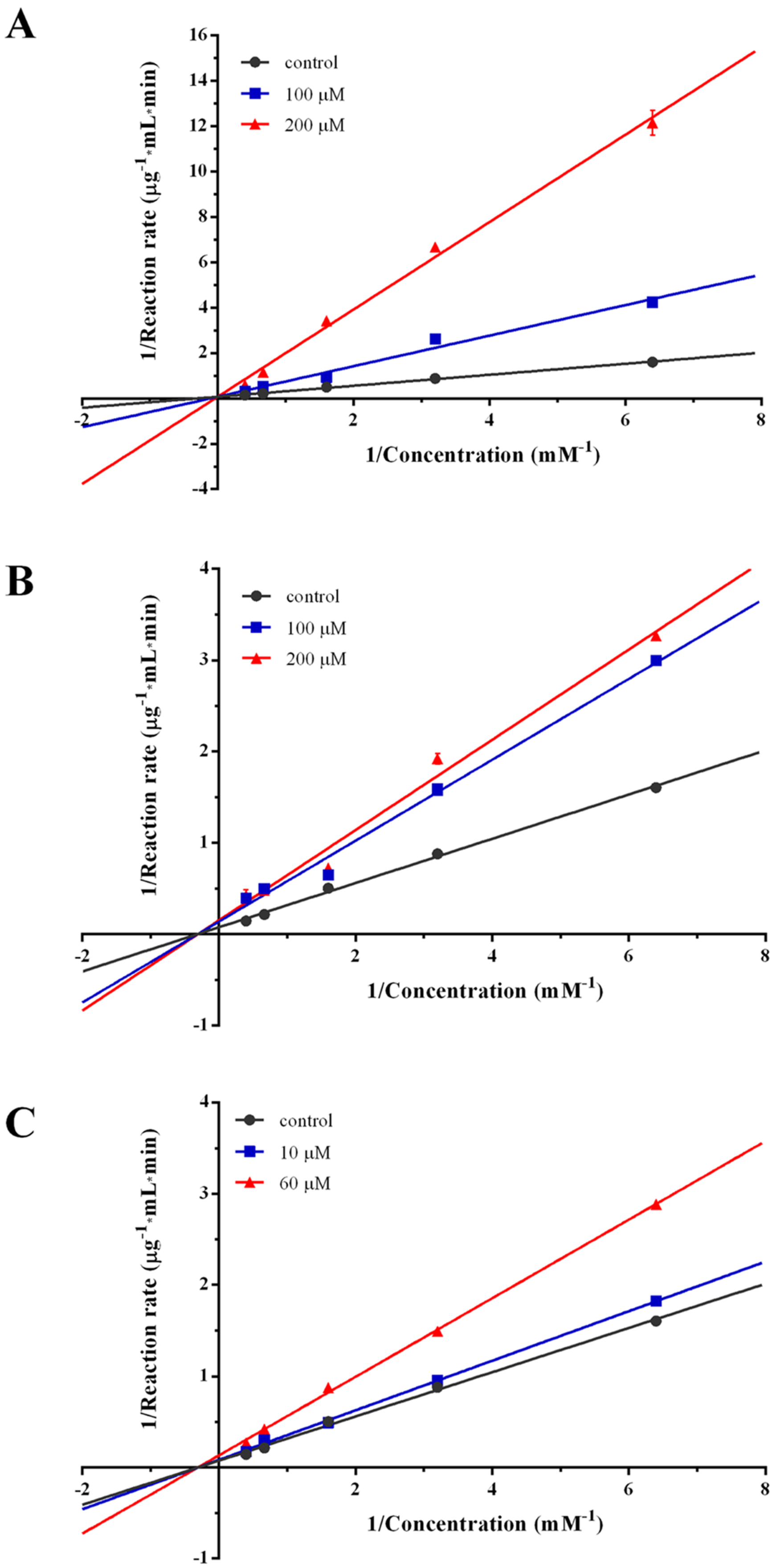

Figure 2. Lineweaver−Burk diagram of pentapeptides obtained from fermented milk (FM) and ultrahigh-pressure-treated FM (UHP-FM). A: HLPLP; B: PYPQR; and C: VAPFP.

https://doi.org/10.1021/acs.jafc.3c03752
J. Agric. Food Chem. XXXX, XXX, XXX−XXX

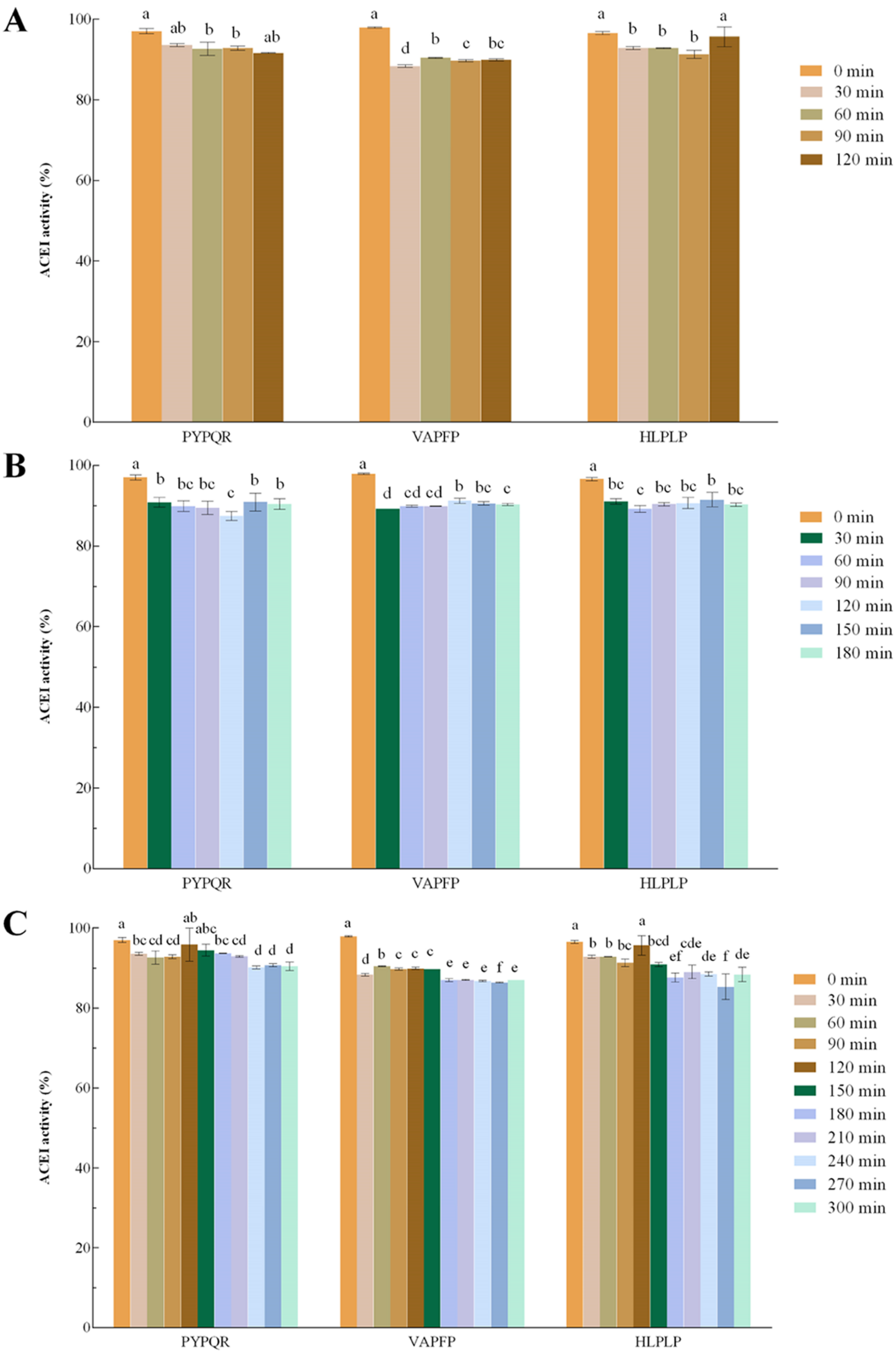

Figure 3. Validation of gastrointestinal stability of FM and UHP-FM-derived angiotensin converting enzyme (ACE) inhibitory (ACEI) peptides. A: pepsin digestion; B: trypsin digestion; and C: gastrointestinal protease digestion. Different letters in the same test indicate significant differences ($P < 0.05$).

Table 3. Results of the Flexible Docking Interaction between Pentapeptides and ACE

	ChiRotor E-total (kcal/mol)	ChiRotor E-elec (kcal/mol)	ChiRotor E-vdw (kcal/mol)	ChiFlex Energy (kcal/mol)	-CDOCKE_ENERGY (kcal/mol)	-CDOCKER_INTERACTION_ENERGY (kcal/mol)	LibDock score
PYPQR	−47.27	−8.63	−49.52	−23.32	75.89	89.79	133.19
VAPFP	−52.65	−8.72	−54.47	−8.32	83.43	107.5	131.73
HLPLP	−44.78	−8.00	−49.51	9.13	80.42	101.31	128.55

https://doi.org/10.1021/acs.jafc.3c03752
J. Agric. Food Chem. XXXX, XXX, XXX−XXX

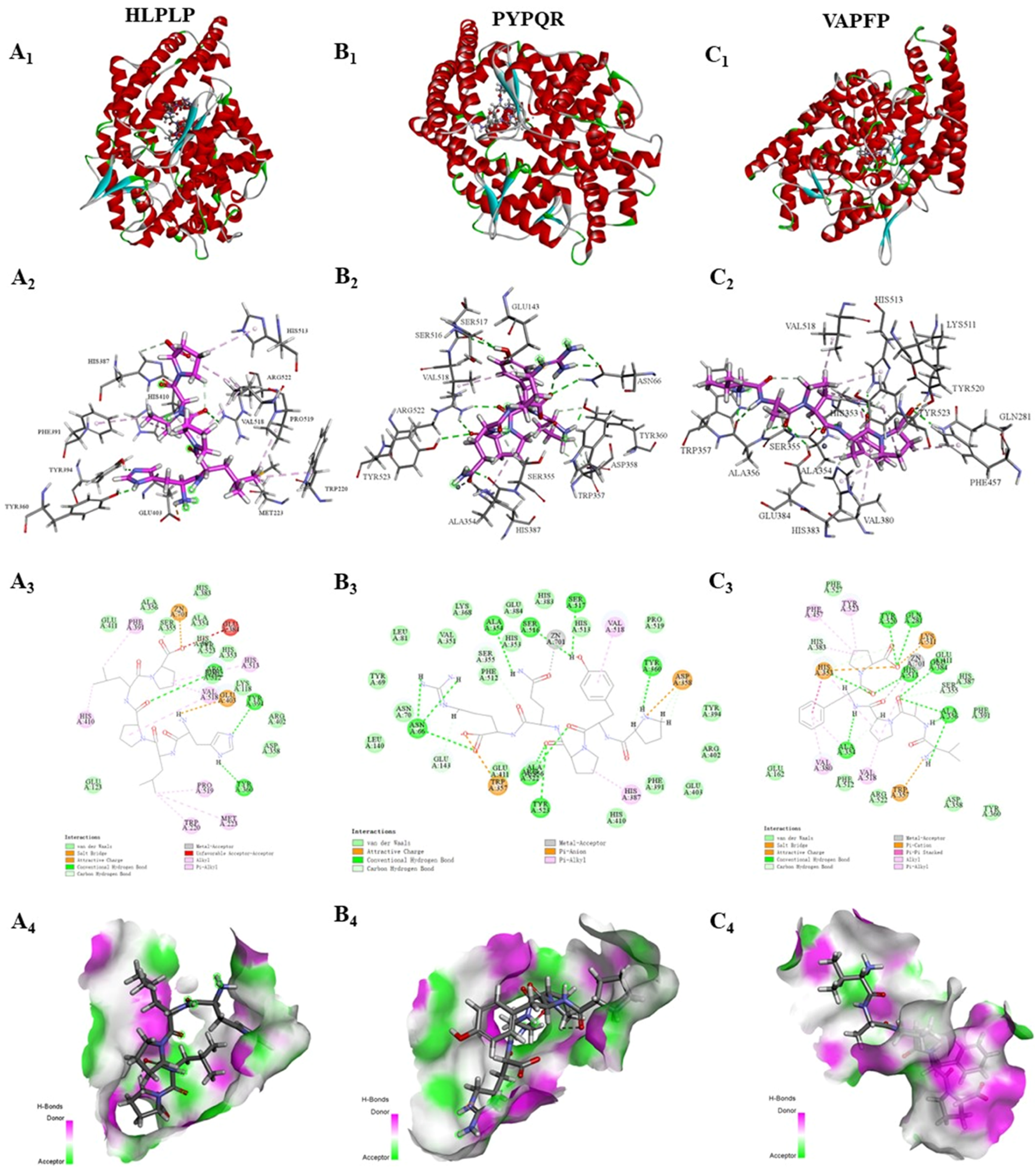

Figure 4. Molecular docking model of the pentapeptides and ACE. A_1, B_1, and C_1: three-dimensional (3D) diagram of docking of the pentapeptides to ACE; A_2, B_2, and C_2: 3D diagram of local interaction of the pentapeptides with the amino acid residues of ACE; A_3, B_3, and C_3: two-dimensional (2D) diagram of interaction of the pentapeptides with the amino acid residues of ACE; and A_4, B_4, and C_4: 3D diagram of the H bond between the pentapeptides and the amino acid residues of ACE.

interaction at the inhibition site. In addition, Zn^{2+} plays an important role in the docking process.[28]

HLPLP (Figure 4A_2,A_3) exhibited three conventional hydrogen bonds with $Tyr394_{2.52\ Å}$, $Arg522_{3.06\ Å}$, and $Tyr360_{2.16\ Å}$ amino acid residues of ACE at various distances, with bond angles of 107.156, 125.453, and 153.054°, respectively. $His387_{2.95\ Å}$ formed a carbon–hydrogen bond with the bond angle of 96.724°, and the hydrogen bond was short, the bond angle was large, and the action was strong.[29] His387 was an important active site on ACE. HLPLP exhibited alkyl hydrophobicity with $Met223_{4.72\ Å}$, $Val518_{5.11\ Å}$, $Pro519_{4.24\ Å}$, and $Val518_{4.68\ Å}$ and π-alkyl hydrophobicity with

https://doi.org/10.1021/acs.jafc.3c03752
J. Agric. Food Chem. XXXX, XXX, XXX−XXX

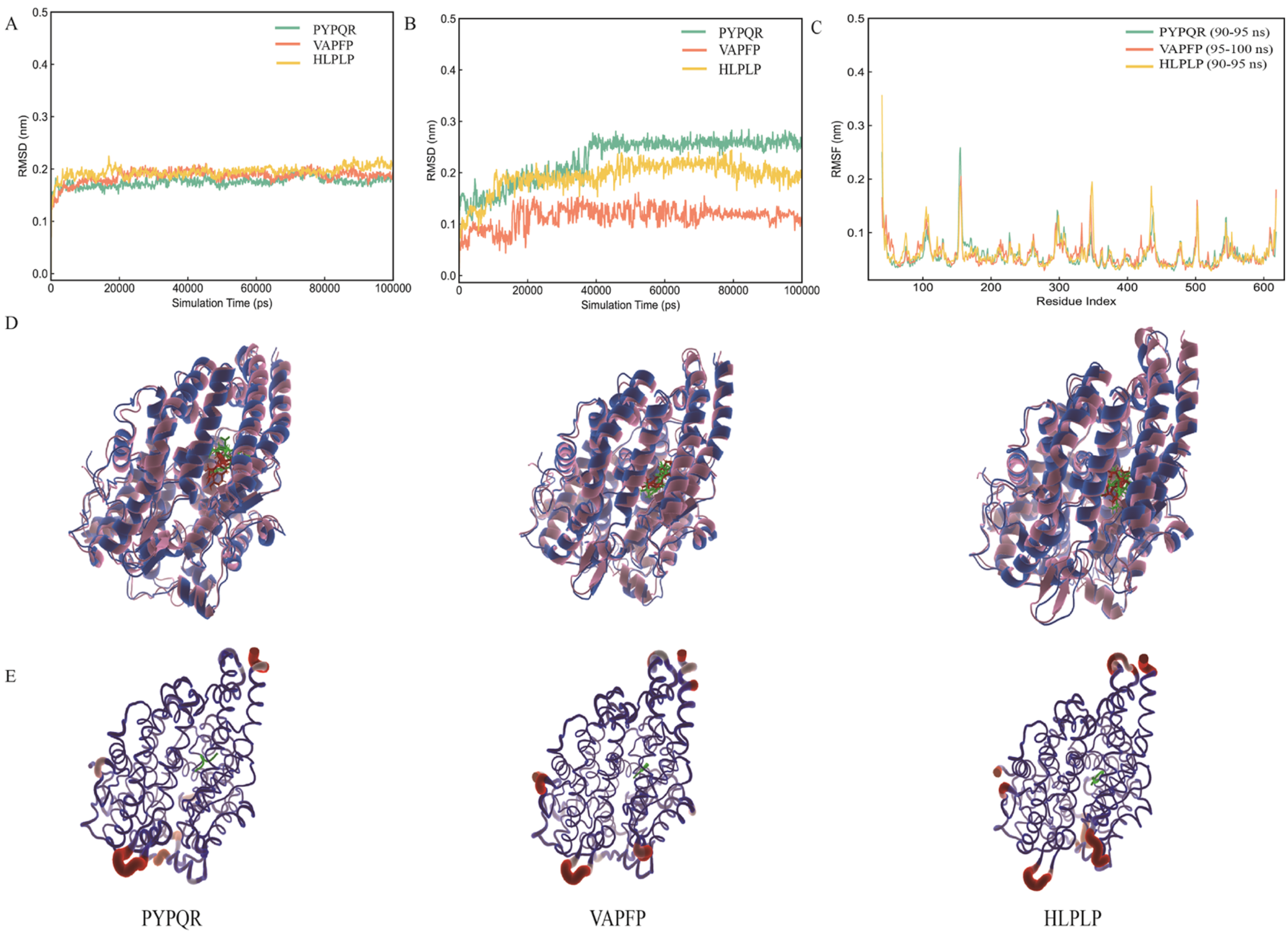

Figure 5. RMSD, RMSF, and β Factor after MD simulation of the FM-derived ACEI peptides. (A) RMSD, (B) RMSD, and (C) RMSF values of the three ACE−peptide systems; (D) structure before (red) and after (blue) MD simulation; and (E) β-factor of the three ACE−peptide systems.

Trp220$_{4.53\ Å}$, Phe391$_{5.01\ Å}$, His410$_{3.66\ Å}$, and His513$_{5.50\ Å}$, with His513 in the S2 pocket. HLPLP and Zn701$_{2.09\ Å}$ exhibited metal receptor interaction and formed a tetrahedral structure, which improved the credibility of docking results and the hit rate of virtual screening. HLPLP and Glu403$_{2.20\ Å}$ formed a salt bridge. Electrostatic interaction existed between HLPLP and Zn701$_{2.24\ Å}$. HLPLP exhibited van der Waals interactions with Glu411, Ala356, His383, Ala354, His387, Tyr512, Phe512, Lys118, Arg402, Asp358, and Glu123.

PYPQR (Figure 4B$_1$,B$_2$) formed conventional hydrogen bonds with the amino acid residues Asn66$_{2.67/2.38/2.09\ Å}$, Arg522$_{2.37/2.39\ Å}$, Tyr523$_{3.01\ Å}$, Tyr360$_{1.94\ Å}$, Ser516$_{2.06\ Å}$, Ser517$_{2.93\ Å}$, and Ala354$_{2.15\ Å}$ of ACE at 10 different distances. The bond angles were 146.664, 129.269, 134.979, 133.886, 153.885, 133.356, 144.642, 128.691, 147.813, and 115.193°, respectively, with Tyr523 and Ala354 in the S1 pocket. PYPQR formed five carbon−hydrogen bonds with Ser355$_{2.45Å}$, Asp358$_{3.07/3.02Å}$, Tyr360$_{2.52Å}$, and Glu143$_{2.55Å}$ at bond angles of 134.466, 107.561, 110.432, 113.828, and 138.761°, respectively. PYPQR exhibited π-alkyl hydrophobic interaction with His387$_{4.73Å}$ and Val518$_{5.17Å}$. PYPQR and Zn701$_{2.01Å}$ exhibited metal receptor interaction. PYPQR exhibited electrostatic interaction with Asp358$_{4.51Å}$ and π-anionic electrostatic interaction with Trp357$_{4.94Å}$ and TRP357$_{4.85Å}$. PYPQR exhibited van der Waals interactions with Asn70, Leu81, Val351, Lys368, Phe512, His353, Glu384, His383, His513, Rro519, Tyr394, Agr402, Glu403, Phe391, His410, Glu411, and Glu143.

VAPFP (Figure 4C$_1$,C$_2$) formed conventional hydrogen bonds with the amino acid residues Gln281$_{2.26Å}$, His353$_{1.94Å}$, Glu384$_{2.95Å}$, His513$_{2.13Å}$, Tyr520$_{2.00Å}$, Ala354$_{2.54Å}$, and Ala356$_{2.16/1.76/2.38Å}$ of ACE at nine different distances, and the angles were 161.278, 152.694, 147.246, 126.063, 128.951, 119.023, 135.932, 153.459, and 124.731°, respectively. Gln281, His353, His513, and Tyr520 were present in the S2 pocket, and Ala354 and Glu384 were present in the S1 oral band. His353 exerted the strongest force. VAPFP formed five carbon−hydrogen bonds with His353$_{2.61Å}$, Ser355$_{2.41Å}$, His513$_{2.68Å}$, Ala354$_{2.23Å}$, and His383$_{2.59Å}$. The bond angles were 140.444, 134.694, 100.979, 128.849, and 153.629°, respectively. His353 and His513 were present in the S2 pocket. Ala354 was present in the S1 pocket. His383 was one of the important active sites of ACE. VAPFP and His353$_{4.35Å}$ of imidazole exhibited $\pi-\pi$ stacking hydrophobic interaction. VAPFP and Val518$_{4.36Å}$ exhibited alkyl hydrophobic interaction. VAPFP exhibited π-alkyl hydrophobic interaction with His353$_{5.49Å}$, His383$_{5.16Å}$, Phe457$_{5.44Å}$, His513$_{5.20Å}$, Tyr523$_{4.73Å}$, Ala354$_{4.08Å}$, and Val380$_{4.29Å}$. VAPFP and Zn701$_{2.00Å}$ exhibited metal receptor interaction with the formation of a tetrahedral structure. The outer layer had 10 electrons, and all five d orbitals were full, with one *s* orbital and three p orbitals. Therefore, sp^3 hybridization was adopted to form a regular

https://doi.org/10.1021/acs.jafc.3c03752
J. Agric. Food Chem. XXXX, XXX, XXX−XXX

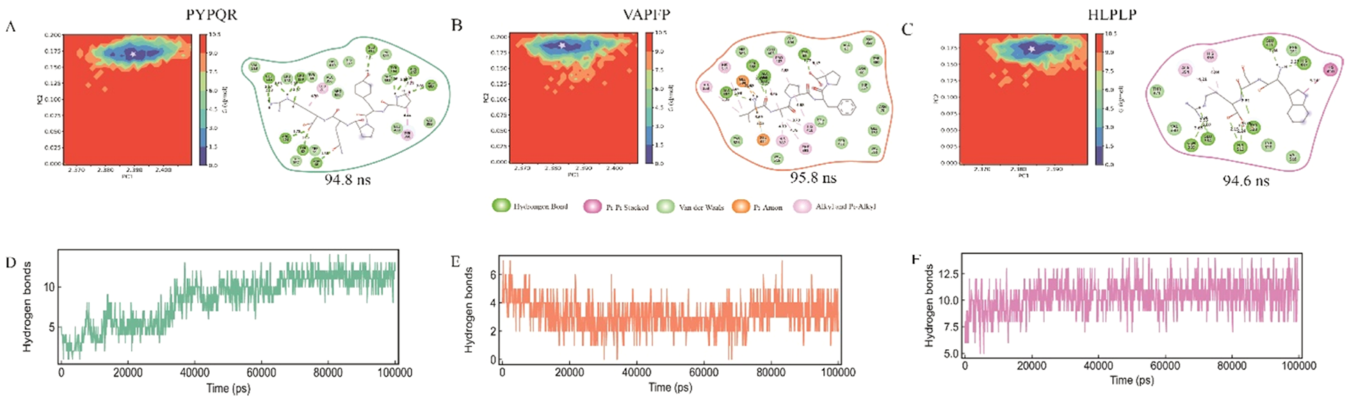

Figure 6. Hydrogen bonds and free energy landscapes of the FM-derived ACEI peptides as revealed by MD. (A−C) Free energy landscapes; and (D−F) hydrogen bonds.

tetrahedral structure, and the acting force was more stable. VAPFP formed a salt bridge with Lys511$_{1.80Å}$. VAPFP exhibited electrostatic interaction with His353$_{4.98Å}$ and π-cationic electrostatic interaction with Trp357$_{3.16/3.80Å}$. The short peptide VAPFP (N1) exhibited π-cationic interaction with indole with a bicyclic structure Trp (W) on ACE. VAPFP exhibited van der Waals interactions with Phe527, Glu411, His387, Phe911, Tyr360, Asp358, Arg522, Phe512, and Glu162. Since the indole in the Trp (W) side chain of the short peptide has a bicyclic structure, this structure may broaden the range of intermolecular interaction. The interaction with His from imidazole can form $\pi-\pi$ stacking, π−cation, and $\pi-\pi$ t-shape, which may be the main factor leading to the improvement of affinity compared with Tyr (Y) with a monocyclic structure. VAPFP acted on Ala354 and Tyr523 in the S1 pocket; Gln281, His353, Lys511, His513, and Tyr520 in the S2 pocket; and Glu162 and Zn^{2+} at the active site His383 and S1′ pocket. The activity of the short peptide of VAPFP may be higher, and its binding to ACE was more stable. Moreover, the distance between the Zn ion and ACEI peptide was close, and its ACEI activity was better.[30] The distance between Zn^{2+} and the peptide exhibited a trend of HLPLP$_{2.09\ Å}$ > PYPQR$_{2.01\ Å}$ > VAPFP$_{2.00\ Å}$, and IC_{50} exhibited a trend of VAPFP > PYPQR > HLPLP.

3.5. Probing the Binding Site by MD Simulation.

Trajectories of the ACE protein backbone converged at approximately 20 and 15 ns. The RMSD values for the three systems fluctuated between 0.10 and 0.22 nm (Figure 5A). Trajectories of all three peptides converged at approximately 40 ns. The RMSD values fluctuated between 0.05 and 0.1 nm for PYPQR, VAPFP, and HLPLP (Figure 5B). These data suggested that all three pentapeptides could stably bind to the active site; however, PYPQR and HLPLP exhibited large fluctuations. Meanwhile, ACE binding with VAPFP reached equilibrium faster than ACE binding with HLPLP or PYPQR, indicating that the combination of ACE and VAPFP sustained more firmly.[31]

In addition, the structure was aligned before (red) and after (blue) the MD simulation (Figure 5D). The protein structures of VAPFP exhibited a small fluctuation; however, PYPQR and HLPLP exhibited large fluctuations. This was consistent with the previous analysis.

The root-mean-square fluctuation (RMSF) was used to describe the freedom of motion of each atom in a molecule. The larger the RMSF, the more flexible the residue. The RMSF plot indicated that the conformation fluctuations of all residues from three ACE−peptide systems were similar (Figure 5C). Under the simulated conditions, the maximum RMSF value was also less than 0.5, which indicated that ACE was relatively stable in the process of complex formation.[32] Most of the fluctuations in the residues of the ring of the ACE during simulation were more flexible than those of the helical region of the ACE. The representative stable structures at 100 ns by the β-factor indicated that the conformational fluctuations of the three systems were similar (Figure 5E).

3.6. Binding Mode of the Three Pentapeptides.

The free energy landscapes (FELs) were used to select the representative conformations of the three systems for binding mode analysis. The FELs were determined as a function of Rg (PC1) and RMSD (PC2), which could find the local lowest energy conformations. As shown in Figure 6, the region marked in darker blue indicated lower energy of structures. According to the results of FELs, the reprehensive structures for the three systems were picked out at PYPQR (94.8 ns, Figure 6A), VAPFP (95.8 ns, Figure 6B), and HLPLP (94.6 ns, Figure 6C). Binding mode analysis revealed that the three peptides exhibited a stable bond with ACE at various degrees. PYPQR formed 12 hydrogen bonds with Tyr62$_{1.65Å}$, Asn66$_{1.86Å}$, Arg124$_{1.78Å}$, Leu139$_{2.37/2.47Å}$, Glu143$_{2.57/2.58Å}$, Asp358$_{2.03Å}$, Tyr394$_{2.08Å}$, Arg402$_{2.30/2.60Å}$, and Glu411$_{2.21Å}$ and hydrophobic interactions with Leu81$_{4.70Å}$, Tyr360$_{4.44Å}$, and Arg402$_{4.71Å}$. The amino acid residue Glu411 plays an important role at the inhibition site of ACE. VAPFP formed five hydrogen bonds with Tyr62$_{1.72Å}$, Ala354$_{2.47Å}$, Ser355$_{2.57Å}$, Ala356$_{1.98Å}$, and Glu411$_{2.13Å}$; eight hydrophobic interactions with Tyr62$_{5.47Å}$, His353$_{5.32Å}$, Ala356$_{4.46Å}$, His387$_{4.19Å}$, Phe391$_{4.78Å}$, Pro407$_{4.93Å}$, His410$_{3.70Å}$, and His513$_{5.44Å}$; and electrostatic interactions with Glu384$_{1.82/2.85Å}$ and Glu411$_{3.69Å}$. VAPFP exhibited a stable effect on Ala354 and Glu384 in the S1 pocket, His513 and His353 in the S2 pocket, and active sites Glu411 and His387 in the simulation process. HLPLP formed eight hydrogen bonds with Gln369$_{2.65Å}$, Glu384$_{2.07/2.55Å}$, His387$_{2.27Å}$, Glu411$_{1.84Å}$, His513$_{2.15/2.24Å}$, and Tyr523$_{2.81Å}$ and three hydrophobic interactions with HIS353$_{4.84Å}$, Ala354$_{4.21Å}$, and His410$_{5.24Å}$. During the simulation, HLPLP exhibited relatively stable effects on Glu384, Tyr523, and Ala354 in the S1 pocket, His353 and His513 in the S2 pocket, and active sites Glu411 and His387.

We studied the pattern of hydrogen bonds between the ACE protein and three pentapeptides. The number of hydrogen bonds formed between the three peptides and ACE was changed (Figure 6), and only the bonds that strictly met the

https://doi.org/10.1021/acs.jafc.3c03752
J. Agric. Food Chem. XXXX, XXX, XXX−XXX

Table 4. Binding Free Energy of Three Systems Calculated by the MM-PBSA Method

	energy[a] (kJ/mol)				
system	ΔG_{bind}	ΔG_{vdw}	ΔG_{ele}	ΔG_{polar}	$\Delta G_{nonpolar}$
PYPQR	−437.1 ± 17.5	−217.2 ± 17.5	−867.0 ± 23.0	683.0 ± 21.4	−36.0 ± 0.6
VAPFP	−63.7 ± 21.1	−208.1 ± 14.1	−336.5 ± 28.3	510.7 ± 30.0	−29.8 ± 0.7
HLPLP	26.8 ± 26.0	−190.1 ± 16.2	−317.9 ± 24.1	567.1 ± 26.9	−32.3 ± 0.7

[a]The average energy is taken from the calculation of 51 frame structures.

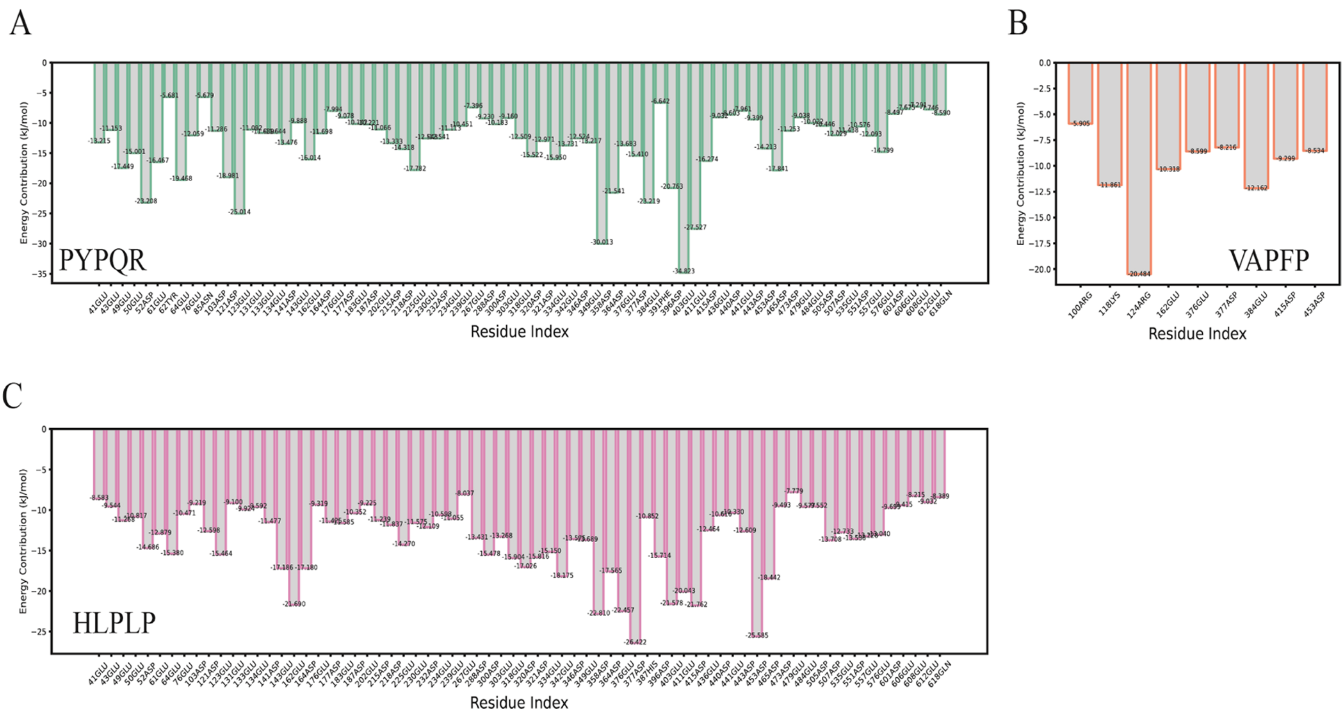

Figure 7. Hydrogen bonds formed by the three ACEI peptides as revealed by MD.

hydrogen bond formation angle and distance remained. The ACE−peptide system formed after 40 ns, 7−15 for the PYPQR hydrogen bond (Figure 6D), 1−7 for the VAPFP hydrogen bond (Figure 6E), and 2−10 for the HLPLP hydrogen bond (Figure 6F). These data indicated that the binding of three peptides to the active sites of ACE was stable, and the binding of PYPQR to ACE exhibited the most stability.

3.7. Calculation of Binding Free Energy. In this study, the binding free energies were effectively estimated using the MM-PBSA method. For each system, 51 snapshots were taken at an interval of 100 ps from the structural ensemble recorded in the MD trajectory during the last 5 ns. The ΔG_{bind} values are given in Table 4. The values of the ΔG_{bind} for PYPQR, VAPFP, and HLPLP were −437.1 ± 17.5, − 63.7 ± 21.1, and 26.8 ± 26.0 kJ·mol^{-1}, respectively. PYPQR exhibited stronger interaction with ACE than VAPFP and HLPLP. Particularly, HLPLP exhibited positive binding energy, indicating poor interaction with ACE. ΔG_{bind} comprise of ΔG_{vdw}, ΔG_{ele}, ΔG_{pol}, and ΔG_{nonpol}. Among them, ΔG_{vdw}, ΔG_{ele}, and ΔG_{nonpol}, but not ΔG_{pol}, were favorable to inhibitor binding.[33] Therefore, the research shows that VAPFP was more conducive to the combination with ACE.

The contribution of residues to the ΔG_{bind} was investigated via energy decomposition analysis for the three systems. Generally, a residue was considered important for ligand binding if its interaction energy with the residue was <−1 kcal/mol. To identify the most important residues contributing to the ΔG_{bind}, the energy threshold was set to −5 kcal·mol^{-1}. For PYPQR (Figure 7A), 73 residues were found to be important. For VAPFP (Figure 7B), 9 residues were found to be important. For HLPLP (Figure 7C), 70 residues were found to be important. Clearly, PYPQR displayed stable interactions with the residues in the active site of the ACE protein.

Three novel angiotensin converting enzyme inhibitory pentapeptides were identified from milk fermented with *L. delbrueckii* QS306 with and without ultrahigh-pressure treatment. Among them, HLPLP, PYPQR, and VAPFP exhibited the most potent ACEI activity, with IC_{50} values of 698.943, 454.0911, and 10.5613 μmol/L, respectively. The inhibition pattern of the pentapeptide HLPLP exhibited competitive inhibition, while PYPQR and VAPFP exhibited noncompetitive inhibition. In addition, after the simulation of gastrointestinal digestion, the ACEI activities of the three pentapeptides were significantly reduced ($P < 0.05$). However, they were greater than 85% after digestion. Molecular docking studies revealed that all three pentapeptides could bind to the key residues at the ACE active site. Further, molecular dynamics (MD) simulation revealed that PYPQR and VAPFP exhibited stronger interaction with ACE. Further studies including in vivo experiments are necessary to investigate the efficacy of VAPFP and PYPQR in controlling blood pressure and their potential use in treating hypertension.

https://doi.org/10.1021/acs.jafc.3c03752
J. Agric. Food Chem. XXXX, XXX, XXX−XXX

■ AUTHOR INFORMATION

Corresponding Authors

Wuhanqimuge − *Experimental Center, Inner Mongolia Traditional Chinese & Mongolian Medical Research Institute, Hohhot, Inner Mongolia 010017, People's Republic of China*; Phone: 18047119596; Email: 939839367@qq.com

Quan Shuang − *Department of College of Food Science and Engineering, Inner Mongolia Agricultural University, Hohhot, Inner Mongolia 010018, People's Republic of China*; Phone: 15849166155; Email: shuangquan@imau.edu.cn

Author

Nan Wu − *Department of College of Food Science and Engineering, Inner Mongolia Agricultural University, Hohhot, Inner Mongolia 010018, People's Republic of China*; orcid.org/0000-0001-8591-9873

Complete contact information is available at:
https://pubs.acs.org/10.1021/acs.jafc.3c03752

Notes

The authors declare no competing financial interest.

■ ACKNOWLEDGMENTS

This work was supported by the Inner Mongolia Natural Science Foundation (grant no. 2021MS03059), the Inner Mongolia Chinese and Mongolian Medicine Young and Middle Aged Leader Project (NEI WEI ZHONG(MENG) CHUAN CHENG ZI[2022]NO.108), and the National Natural Science Foundation of China-Young Foundation (grant no. 82204377). We thank Shanghai Bioprofile Technology Company Ltd. for the peptide sequence analysis using UPLC-Q-exactive-HF-X-MS/MS.

■ ABBREVIATIONS

ACE, angiotensin converting enzyme; MD, molecular dynamics; SBP, systolic blood pressure; DBP, diastolic blood pressure; HA, hippuric acid; HHL, *N*-hippuryl-His-Leu hydrate; MRS, de Man, Rogosa, and Sharpe; UF, ultrafiltration; MW, molecular weight; BBS, boric acid buffer solution; EM, energy minimization; RMSD, root-mean-square deviation; RMSF, root-mean-square fluctuation; FEL, free energy landscape; MM-PBSA, molecular mechanics Poisson−Boltzmann surface area

■ REFERENCES

(1) Egan, B. M.; Zhao, Y. Different definitions of prevalent hypertension impact: the clinical epidemiology of hypertension and attainment of Healthy People goals. *J. Clin Hypertens* **2013**, *15* (3), 154−61.

(2) Ezzati, M.; Lopez, A. D.; Rodgers, A.; Vander Hoorn, S.; Murray, C. J. Selected major risk factors and global and regional burden of disease. *Lancet* **2002**, *360* (9343), 1347−60.

(3) Kearney, P. M.; Whelton, M.; Reynolds, K.; Muntner, P.; Whelton, P. K.; He, J. Global burden of hypertension: analysis of worldwide data. *Lancet* **2005**, *365* (9455), 217−23.

(4) Bakris, G. L.; Frohlich, E. D. The evolution of antihypertensive therapy: an overview of four decades of experience. *J. Am. Coll. Cardiol.* **1989**, *14* (7), 1595−608.

(5) Kotchen, T. A. Historical trends and milestones in hypertension research: a model of the process of translational research. *Hypertension* **2011**, *58* (4), 522−38.

(6) White, W. B. Update on the drug treatment of hypertension in patients with cardiovascular disease. *Am. J. Med.* **2005**, *118* (7), 695−705.

(7) Ko, D. T.; Hebert, P. R.; Coffey, C. S.; Curtis, J. P.; Foody, J. M.; Sedrakyan, A.; Krumholz, H. M. Adverse effects of beta-blocker therapy for patients with heart failure: a quantitative overview of randomized trials. *Arch. Intern. Med.* **2004**, *164* (13), 1389−94.

(8) Brown, N. J.; Vaughan, D. E. Angiotensin-converting enzyme inhibitors. *Circulation* **1998**, *97* (14), 1411−20.

(9) Ondetti, M. A.; Cushman, D. W. Angiotensin-converting enzyme inhibitors: biochemical properties and biological actions. *Crit. Rev. Biochem.* **1984**, *16* (4), 381−411.

(10) Ondetti, M. A.; Williams, N. J.; Sabo, E. F.; Pluscec, J.; Weaver, E. R.; Kocy, O. Angiotensin-converting enzyme inhibitors from the venom of Bothrops jararaca. Isolation, elucidation of structure, and synthesis. *Biochemistry* **1971**, *10* (22), 4033−9.

(11) Yamamoto, N. Antihypertensive peptides derived from food proteins. *Biopolymers* **1997**, *43* (2), 129−34.

(12) Ariyoshi, Y. Angiotensin-converting enzyme inhibitors derived from food proteins. *Trends Food Sci. Technol.* **1993**, *4* (5), 139−144.

(13) Wu, N.; Xu, W.; Liu, K.; Xia, Y. Shuangquan, Angiotensin-converting enzyme inhibitory peptides from Lactobacillus delbrueckii QS306 fermented milk. *J. Dairy Sci.* **2019**, *102* (7), 5913−5921.

(14) Tu, M.; Cheng, S.; Lu, W.; Du, M. Advancement and prospects of bioinformatics analysis for studying bioactive peptides from food-derived protein: Sequence, structure, and functions. *TrAC, Trends Anal. Chem.* **2018**, *105*, 7−17.

(15) Caballero, J. Considerations for Docking of Selective Angiotensin-Converting Enzyme Inhibitors. *Molecules* **2020**, *25* (2), No. 295, DOI: 10.3390/molecules25020295.

(16) Xu, Z.; Wu, C.; Sun-Waterhouse, D.; Zhao, T.; Waterhouse, G. I. N.; Zhao, M.; Su, G. Identification of post-digestion angiotensin-I converting enzyme (ACE) inhibitory peptides from soybean protein Isolate: Their production conditions and in silico molecular docking with ACE. *Food Chem.* **2021**, *345*, 128855.

(17) Cox, J.; Neuhauser, N.; Michalski, A.; Scheltema, R. A.; Olsen, J. V.; Mann, M. Andromeda: a peptide search engine integrated into the MaxQuant environment. *J. Proteome Res.* **2011**, *10* (4), 1794−805.

(18) Wu, N.; Zhang, F.; Shuang, Q. Peptidomic analysis of the angiotensin-converting-enzyme inhibitory peptides in milk fermented with Lactobacillus delbrueckii QS306 after ultrahigh pressure treatment. *Food Res. Int.* **2023**, *164*, No. 112406.

(19) Wu, N.; Zhao, Y.; Wang, Y.; Shuang, Q. Effects of ultra-high pressure treatment on angiotensin-converting enzyme (ACE) inhibitory activity, antioxidant activity, and physicochemical properties of milk fermented with *Lactobacillus delbrueckii* QS306. *J. Dairy Sci.* **2022**, *105* (3), 1837−1847.

(20) Sun, M.-L.; Zhang, Q.; Ma, Q.; Fu, Y.-H.; Jin, W.-G.; Zhu, B.-W. Affinity purification of angiotensin-converting enzyme inhibitory peptides from Volutharpa ampullacea perryi protein hydrolysate using Zn-SBA-15 immobilized ACE. *Eur. Food Res. Technol.* **2018**, *244* (3), 457−468.

(21) Zhu, C.-Z.; Zhang, W.-G.; Kang, Z.-L.; Zhou, G.-H.; Xu, X.-L. Stability of an antioxidant peptide extracted from Jinhua ham. *Meat Sci.* **2014**, *96* (2, Part A), 783−789.

(22) Prakash Nirmal, N.; Singh Rajput, M.; Bhojraj Rathod, N.; Mudgil, P.; Pati, S.; Bono, G.; Nalinanon, S.; Li, L.; Maqsood, S. Structural characteristic and molecular docking simulation of fish protein-derived peptides: Recent updates on antioxidant, anti-hypertensive and anti-diabetic peptides. *Food Chem.* **2023**, *405* (Pt A), 134737.

(23) Ma, F. F.; Wang, H.; Wei, C. K.; Thakur, K.; Wei, Z. J.; Jiang, L. Three Novel ACE Inhibitory Peptides Isolated From Ginkgo biloba Seeds: Purification, Inhibitory Kinetic and Mechanism. *Front. Pharmacol.* **2018**, *9*, No. 1579.

(24) Ko, J.-Y.; Kang, N.; Lee, J.-H.; Kim, J.-S.; Kim, W.-S.; Park, S.-J.; Kim, Y.-T.; Jeon, Y.-J. Angiotensin I-converting enzyme inhibitory peptides from an enzymatic hydrolysate of flounder fish (Paralichthys

olivaceus) muscle as a potent anti-hypertensive agent. *Process Biochem.* **2016**, *51* (4), 535−541.

(25) Guo, M.; Chen, X.; Wu, Y.; Zhang, L.; Huang, W.; Yuan, Y.; Fang, M.; Xie, J.; Wei, D. Angiotensin I-converting enzyme inhibitory peptides from Sipuncula (Phascolosoma esculenta): Purification, identification, molecular docking and antihypertensive effects on spontaneously hypertensive rats. *Process Biochem.* **2017**, *63*, 84−95, DOI: 10.1016/j.procbio.2017.08.009.

(26) Zhao, T. T.; Zheng, L.; Zhang, Q.; Wang, S. G.; Zhao, Q. Z.; Su, G. W.; Zhao, M. M. Stability towards the gastrointestinal simulated digestion and bioactivity of PAYCS and its digestive product PAY with cognitive improving properties. *Food Funct.* **2019**, *10* (5), 2439−2449.

(27) Ngoh, Y. Y.; Gan, C. Y. Identification of Pinto bean peptides with inhibitory effects on α-amylase and angiotensin converting enzyme (ACE) activities using an integrated bioinformatics-assisted approach. *Food Chem.* **2018**, *267*, 124−131.

(28) Wang, X.; Wu, S.; Xu, D.; Xie, D.; Guo, H. Inhibitor and substrate binding by angiotensin-converting enzyme: quantum mechanical/molecular mechanical molecular dynamics studies. *J. Chem. Inf Model* **2011**, *51* (5), 1074−82.

(29) Kobko, N.; Paraskevas, L.; del Rio, E.; Dannenberg, J. J. Cooperativity in Amide Hydrogen Bonding Chains: Implications for Protein-Folding Models. *J. Am. Chem. Soc.* **2001**, *123* (18), 4348−4349.

(30) Abdelhedi, O.; Nasri, R.; Mora, L.; Jridi, M.; Toldrá, F.; Nasri, M. In silico analysis and molecular docking study of angiotensin I-converting enzyme inhibitory peptides from smooth-hound viscera protein hydrolysates fractionated by ultrafiltration. *Food Chem.* **2018**, *239*, 453−463.

(31) Yan, W.; Lin, G.; Zhang, R.; Liang, Z.; Wu, L.; Wu, W. Studies on molecular mechanism between ACE and inhibitory peptides in different bioactivities by 3D-QSAR and MD simulations. *J. Mol. Liq.* **2020**, *304*, 112702.

(32) Feng, X.; Liao, D.; Sun, L.; Feng, S.; Wu, S.; Lan, P.; Wang, Z.; Lan, X. Exploration of interaction between angiotensin I-converting enzyme (ACE) and the inhibitory peptide from Wakame (Undaria pinnatifida). *Int. J. Biol. Macromol.* **2022**, *204*, 193−203.

(33) Zhang, H.; Luo, Q.-Q.; Hu, M.-L.; Wang, N.; Qi, H.-Z.; Zhang, H.-R.; Ding, L. Discovery of potent microtubule-destabilizing agents targeting for colchicine site by virtual screening, biological evaluation, and molecular dynamics simulation. *Eur. J. Pharm. Sci.* **2023**, *180*, No. 106340.

https://doi.org/10.1021/acs.jafc.3c03752
J. Agric. Food Chem. XXXX, XXX, XXX−XXX